PAUL SCHERRER INSTITUT

PSI Bericht Nr. 03-05
November 2002
ISSN 1019-0643

Nuclear Energy and Safety Research Department

On the Decay Ratio Determination in BWR Stability Analysis by Auto-Correlation Function Techniques

Klaus Behringer* and Dieter Hennig

* Guest scientist at PSI

On the Decay Ratio Determination in BWR Stability Analysis by Auto-Correlation Function Techniques

K. Behringer [*] and D. Hennig
Paul Scherrer Institute (PSI)

Nuclear Energy and Safety Department

Würenlingen and Villigen

November 2002

[*]Guest scientist at PSI

Abstract

A novel auto-correlation function (ACF) method has been investigated for determining the oscillation frequency and the decay ratio in BWR stability analyses. The neutron signals are band-pass filtered to separate the oscillation peak in the power spectral density (PSD) from background. Two linear second–order oscillation models are considered. These models, corrected for signal filtering and including a background term under the peak in the PSD, are then least-squares fitted to the ACF of the previously filtered neutron signal, in order to determine the oscillation frequency and the decay ratio. Our method uses fast Fourier transform techniques with signal segmentation for filtering and ACF estimation. Gliding 'short-term' ACF estimates on a record allow the evaluation of uncertainties. Numerical results are given which have been obtained from neutron data of the recent Forsmark I and Forsmark II NEA benchmark project. Our results are compared with those obtained by other participants in the benchmark project. The present PSI report is an extended version of the publication K. Behringer, D. Hennig "A noval auto-correlation function method for the determination of the decay ratio in BWR stability studies" (Behringer, Hennig, 2002).

The FORTRAN codes are described in (Behringer 2001).

Zusammenfassung

Eine neuartige Auto-Correlationsfunktion (ACF) Methode für die Bestimmung der Oscillationsfrequenz und des Abklingverhältnisses in BWR Stabilitätsanalysen wurde untersucht. Die Neutronensignale werden mit einem Bandpass gefiltert, um den Oscillationspeak in der spektralen Leistungsdichte (PSD) vom Untergrund zu separieren. Zwei lineare Oscillationsmodelle zweiter Ordnung werden betrachtet. Die ACF von jedem Modell, welches in Bezug auf die Signalfilterung korrigiert wird und einen Untergrundterm unter dem Peak in der PSD berücksichtigt, wird mit einem Least-Squares Fit an die ACF angepasst, welche an dem zuvor gefilterten Neutronensignal geschätzt wurde, um die Oscillationsfrequenz und das Abklingverhältnis zu bestimmen. Die Verfahren der Signalfilterung und der ACF Schätzung benützen die schnelle Fourier Transformation mit Signalsegmentierung. Gleitende „Kurzzeit" ACF Schätzungen entlang einer Signalaufzeichnung erlauben die Evaluierung von Unsicherheiten. Es werden Resultate dargestellt die für Messsignale der Inkerninstrumentierung des KKW Forsmark (Conde et al, 2001) erhalten worden sind. Sie werden mit jenen von anderen Teilnehmern am Benchmarkprojekt, welche verschiedene andere Analysenmethoden benützten, verglichen. Der PSI Bericht ist eine erweiterte Fassung der Publikation "A noval auto-correlation function method for the determination of the decay ratio in BWR stability studies" (Behringer, Hennig, 2002).

Die FORTRAN Programme sind im Detail im PSI-Bericht (Behringer 2001) beschreiben.

TABLE OF CONTENTS

1. Introduction

In the stability analysis of boiling water reactors (BWRs), most experimental methods use parametric modelling of the neutron signals. The auto-correlation function (ACF) method is non-parametric, but requires the interpretation by a theoretical model. The classical ACF method is based on the linear second-order damped oscillator model. If it is applied to the digital neutron signal data offered by the recent Forsmark I and Forsmark II NEA benchmark project on BWR stability analysis (Conde et al., 2001), the determination of the oscillation frequency and the decay ratio from the first few minima and maxima in ACF estimates failed. This suggested that a more sophisticated ACF method had to be found.

The reason for the failure lay in the background noise. Signal data must be band-pass filtered to separate out the interesting oscillation peak in the power spectral density (PSD). The choice of the filter cutoff frequencies requires initially a PSD estimation. Additionally, a background term under the peak in the PSD must be taken into account. Signal filtering and the inclusion of this PSD background term require a correction of the assumed model ACF. The corrected model ACF is then least-squares fitted to the ACF estimated from the previously filtered signal data. The fitting procedure contains a variable lag-time range (fitting range) parameter. Special techniques have been applied to the filtering procedure and the ACF estimation. Both are based on signal segmentation and the use of the fast Fourier transform (FFT) algorithm. An FFT filter has been developed which approximates the shape of an ideal rectangular band-pass filter. The ACF estimation uses the indirect method with zero-padding.

A modification of this method allows an ACF estimation to be made over an arbitrary number of successive signal segments. A gliding segment analysis (GLSA) has been introduced. 'Short-term' ACF estimates move over the signal length, each forward shifted by one segment. The least-squares fitting is then repetitively applied to each ACF estimate. Average values of the oscillation frequency, the decay ratio, and their standard deviations can be calculated for each specified fitting range, and a criterion has been found which permits the determination of the optimum fitting range. The GLSA allows an uncertainty analysis to be made of the estimate of each fitting parameter and other data derived from them.

The Paul Scherrer Institute (PSI) participated in the benchmark project with parametric signal modelling methods. It was felt, however, that a completely independent and different method should also be available, for data validation. This was the starting point for the development of the present ACF method. Since our investigations and the development of codes could not be finished within the time-table of the benchmark project, only a few, very preliminary, results could be sent to the benchmark project committee.

The international benchmark project revealed that many different methodologies are used at present in the field of signal analysis, and the uncertainties contained within the various approaches are in some cases very different. Hence, PSI has now developed a code containing seven time-series analysis approaches (including the present method) for the calculation of the linear stability characteristics with respect to oscillation frequency and decay ratio (Askari et al., 2001).

Our present report is concerned with the methodology of our ACF method and includes numerical results of the method investigation. It supplements the earlier PSI report by Behringer (2001), which describes the Fortran codes used and developed for this method.

The paper is divided into the following Sections:

In Section 2, we give the theoretical background of our ACF method. Two linear second-order oscillator models are considered. Section 3 summarises our methods applied to signal filtering and the ACF estimation procedure. In Section 4, we explain our fitting procedure and give some details which are believed to be important. Section 5 is concerned with numerical results: the selected examples are compared and discussed with other results from the benchmark project. Finally, concluding remarks are given in Section 6.

2. Theoretical Considerations and Models

The dynamic behaviour of a BWR is non-linear. Following the summary given in a recent paper by Hennig (1999), the feedback of the thermal-hydraulic variables (volumetric steam content, fuel temperature) on the neutron density leads to non-linear terms in the defining equations, because one of the hydraulic balance equations is itself non-linear. In particular, non-linear feedback can induce oscillatory solutions under certain combinations of parameter. Such phenomena can appear as global or regional oscillations. The decay ratio (DR) is used in many cases for characterising these oscillations.

Auto-regressive moving-average (ARMA) modelling of measured neutron signals is a linear approach. The optimal model order can be obtained from the application of an extended Akaike criterion, which was originally developed for auto-regressive (AR) modelling. Under stable operating conditions, all poles of the transfer function must lie within the unit cycle in the z-transform. For the determination of the DR, one must not presume that the system response can be represented by simple periodic functions. It is only necessary that the pulse response of the system is an oscillating function, decaying in time. This is described in the frequency domain by a broken rational transfer function. The DR is determined from the smallest decay constant. Near to a stable fixed-state point in the system equations, non-linear systems behave in a similar way to those which are linear (Guggenheimer and Holmes, 1984), and for these cases the DR can principally be used for characterising the stability properties.

The ACF method is based on the approach of extracting the requested information by a simple, decaying periodic function. PSD estimations on the benchmark data show distortions mainly around the main peak, in particular on the left-hand side. Such distortions also appear then in ACF estimations and make it impossible to read the DR simply from the first few minima and maxima. Our analysis method is based on signal filtering and taking a PSD background term into account. We consider two oscillator models which have been applied by least-squares fitting to the experimental ACFs estimated from previously filtered signal data. These oscillator models are linear and of second order. ARMA modelling of unfiltered neutron signals lead mostly to high orders suggesting that corresponding ACFs behave as resulting from higher order systems. However, since the DR is defined as asymptotic value with the smallest decay constant, the use of second-order models is believed to be quite appropriate in combination with signal filtering.

The oscillation frequency in all benchmark data is near to 0.5 Hz. The digital benchmark records have been sampled at 25 Hz and reduced to an effective sampling frequency of 12.5 Hz. The Nyquist cutoff frequency is 6.25 Hz. We have to assume that the neutron signals have been correctly digitized with preceding anti-aliasing filters. Otherwise, one can argue that, in the absence of any oscillations, measured neutron PSDs are flat up to about 1 Hz, where they show a break point, after which they decay rapidly. This feature is due to propagating void fluctuations and can be explained by a space-energy dependent treatment, which leads to the global-local neutron noise concept in BWR neutron noise analysis (Kosa'ly, 1980). At a sampling frequency of 25 Hz, which is of the order of the roll-off frequency region of the neutron signal amplifiers, a local power range monitor (LPRM) sees only the weak local neutron noise field of a few centimetres in diameter. Aliasing effects are therefore expected to be very small.

The background considered under the oscillation peak in the PSD, is an intrinsic noise part due to the global neutron noise component (possibly in the frequency transition region to the local neutron noise component). It is always present. The appearance of damped oscillations is regareded as a superposed randomly excited independent process, for which the following two oscillator models have been investigated.

2.1 Model A : Linear Second-Order Damped Oscillator

The application of this model to BWR stability analysis is as old as the BWR itself since its development period (Thie, 1981). It is used in the frequency domain by PSD estimations in a rather engineering sense. The transfer function (written in dimensionless form) is given by:

$$H(\omega) = \frac{\omega_0^2}{\omega_0^2 - \omega^2 + 2i\lambda\omega} \tag{1}$$

The frequencies ω and ω_0 are denoted in angular units, ω_0 is the undamped resonance frequency, and λ (>0) is the damping constant which appears in the model ACF as a decay constant. $H(\omega)$ shows resonance behaviour with the oscillation frequency ω_c if:

$$\omega_c^2 = \omega_0^2 - \lambda^2 > 0 \tag{2}$$

If it is assumed that the oscillator is driven by random forces which are white over the resonance frequency region, the ideal PSD follows from:

$$S_{xx}(\omega) = A_0 \frac{\omega_0^4}{(\omega^2 - \omega_0^2)^2 + 4\lambda^2\omega^2} \tag{3}$$

where A_0 is a constant and represents the PSD of the driving forces. However, the peak maximum appears at a third frequency. The peak resonance frequency, ω_r, is given by:

$$\omega_r^2 = \omega_0^2 - 2\lambda^2 > 0 \tag{4}$$

The existence of a real ω_r requires a stronger condition for resonance behaviour than given by Equation (2).

One can calculate the half-power bandwidth $\Delta\omega$ of $S_{xx}(\omega)$. If $\lambda^2 << \omega_0^2$, $\Delta\omega$ is given by the expression $\Delta\omega \approx 2\lambda$. However, in the PSD estimation, peaks are biased, and the magnitude of λ can only be very subjectively estimated. (For our PSD estimations, we used the well-known Welch method (Welch, 1967), with uniform signal window, which leads to the highest peak resolution, but the highest side-lobe level.)

The ideal ACF follows from Equation (3) by the inverse Fourier transform:

$$R_{xx}^{(I)}(\tau) = C_0 e^{-\lambda|\tau|}\left[\cos(\omega_c\tau) + \frac{\lambda}{\omega_c}\sin(\omega_c|\tau|)\right] \tag{5}$$

where τ is the lag time, C_0 is a constant, and the relationship between A_0 and C_0 is:

$$A_0 = \frac{4\lambda}{\omega_0^2} C_0 \tag{6}$$

We define the decay ratio, DR, by:

$$DR = e^{-2\pi\lambda/\omega_c} \tag{7}$$

If the signal data are filtered by an ideal rectangular bandpass filter of unity gain, which has the lower cutoff frequency ω_L and the upper cutoff frequency ω_H, under the condition $\omega_L < \omega_r < \omega_H$, the ACF to be corrected for signal filtering, $R_{xx}^{(C)}(\tau)$, follows from:

$$R_{xx}^{(C)}(\tau) = \frac{1}{\pi} \int_{\omega_L}^{\omega_H} d\omega S_{xx}(\omega) \cos(\omega\tau) \tag{8}$$

The integral must be solved numerically. An attempt to perform an analytical integration leads to exponential integral functions (or associated functions), and the resulting formulae were not very easy to program. Since, for high DR values, $S_{xx}(\omega)$ peaks strongly at ω_r, numerical integration routines cannot solve the problem. Equation (8) has to be rewritten as:

$$R_{xx}^{(C)}(\tau) = R_{xx}^{(I)}(\tau) - \frac{1}{\pi}\left(\int_0^{\omega_L} + \int_{\omega_H}^{\infty} \right) d\omega S_{xx}(\omega) \cos(\omega\tau) \tag{9}$$

The terms within the integrals represent the corrections to be made to the ideal ACF.

For establishing the fitting ACF, $R_{xx}^{(F)}(\tau)$, we add a background ACF, $B(\tau)$:

$$R_{xx}^{(F)}(\tau) = R_{xx}^{(C)}(\tau) + B(\tau) \tag{10}$$

where $B(\tau)$ is given by:

$$B(\tau) = \frac{1}{\pi} \int_{\omega_L}^{\omega_H} d\omega B(\omega) \cos(\omega\tau) \tag{11}$$

Most PSD estimates showed an exponentially decreasing background under the peak, suggesting for $B(\omega)$ the form:

$$B(\omega) = B_0 e^{-\alpha(\omega-\omega_L)}; \omega_L \le \omega \le \omega_H, \alpha > 0 \tag{12}$$

where α and B_0 are constants. We then obtain for $B(\tau)$:

$$B(\tau) = \frac{B_0}{\pi} \left\{ \frac{\alpha}{\alpha^2+\tau^2} \left[\cos(\omega_L\tau) - e^{-\alpha(\omega_H-\omega_L)} \cos(\omega_H\tau) \right] - \frac{\tau}{\alpha^2+\tau^2} \left[\sin(\omega_L\tau) - e^{-\alpha(\omega_H-\omega_L)} \sin(\omega_H\tau) \right] \right\} \tag{13}$$

The case of α=0 (constant background under the peak in the PSD) does not make sense physically. It only leads to a peaking of $R_{xx}^{(F)}(\tau)$ at τ=0, and approaches the Dirac Delta function for $\omega_L \to 0$ and $\omega_H \to \infty$.

$R_{xx}^{(F)}(\tau)$ is the model function which has to be least-squares fitted to the experimental ACF resulting from previously filtered signal data. Natural fitting parameters are C_0 , ω_c , λ , B_0 and α. The DR can then be obtained from λ and ω_c. We provided three options in our fitting codes with respect to the background treatment:

– IBGR = 0 : Three-parameter fit with $B_0 = 0$.

– IBGR = 1 : Four-parameter fit, including B_0 as a fitting parameter, but with a fixed value of α. The value of α can be approximately obtained from a logarithmic plot of the PSD via a slope index, S, which is defined by:

$$S = \log \frac{B(\omega_L + 2\pi)}{B(\omega_L)} \tag{14}$$

For example, a slope index S = -2 means that the background under the peak decays exponentially by 2 decades within 1 Hz.

In order to have a simple criterion for deciding whether the background is small or large, our fitting codes calculate the peak maximum P_{max} in the ideal PSD from the fitting parameter values by:

$$P_{max} = S_{xx}(\omega_r) \tag{15}$$

and the background amplitude, B_{0p} , at ω_r by:

$$B_{0p} = B_0 e^{-\alpha(\omega_r - \omega_L)} \tag{16}$$

The values B_0 at ω_L and $B_{0p} + P_{max}$ at ω_r can then be compared with those in the PSD plot (if the peak width is not very small; otherwise the peak amplitude is strongly biased).

– IBGR = 2 : five-parameter fit, including B_0 and α as fitting parameters. Such a fit, however, is dangerous if the background term is small, as $|B_0|$ and α can then become very large.

It is obvious that the fitting parameters require reasonable initial values (Section 4.1). We distinguish three types of signal filtering:

No filtering: $\omega_L = 0$ (but with DC component removed), ω_H = Nyquist cutoff frequency.

Weak filtering: $0 < \omega_L << \omega_r << \omega_H <$ Nyquist cutoff frequency.

Strong filtering: $0 << \omega_L < \omega_r < \omega_H <<$ Nyquist cutoff frequency. The filter bandwidth is not allowed to be very small. It is well known that signal filtering is connected with a loss of information, requiring a compromise to be made in choosing the filter limits. The peak in the PSD should lie well within the filter cutoff frequencies. Only left-hand-side and right-hand-side distortions (as far as they are visible) should be removed. If a broad (mostly structured) peak appears to be composed of two unresolvable peaks, a separation is not possible and the method fails.

2.2 Model B : Modified Second-Order Oscillator

The appearance of three characteristic frequencies in model A is mathematically correct under the assumption of driving forces which have white noise characteristics (Bendat and Piersol, 1971). It happened many times, in cases with small DR values, that imaginary values of ω_r occurred in the fitting procedure. Model B avoids this problem by considering a slightly modified version of an active second-order resonance filter given in the textbook of Moschytz and Horn (1983). The transfer function reads:

$$H(\omega) = \left(\frac{1}{Q_R} + \frac{i\omega}{\omega_0} + \frac{\omega_0}{i\omega} \right)^{-1} \tag{17}$$

where ω_0 is the resonance frequency, and Q_R the resonance quality factor. The filter exhibits resonance behaviour if $Q_R > 0.5$. Again, if it is assumed that the driving forces are random and white in the resonance frequency region, the ideal PSD is given by:

$$S_{xx}(\omega) = A_0 \frac{\omega_0^2 \omega^2}{(\omega^2 - \omega_0^2)^2 + 4\lambda^2\omega^2} \tag{18}$$

where one can identify:

$$\lambda = \frac{\omega_0}{2Q_R} \tag{19}$$

A remarkable property of this PSD is that the peak amplitude appears exactly at ω_0 and is not affected by Q_R. Hence, we have $\omega_r = \omega_0$ in this model. The half-power frequency points ω_1 and ω_2 are given by:

$$\omega_{1,2}^2 = \frac{\omega_0^2}{2Q_R^2}\left(1 + 2Q^2 \mp \sqrt{1 + 4Q_R^2}\right) \tag{20}$$

from which the half-power bandwidth can be obtained to a very good approximation (for about $Q_R > 2$) by:

$$\Delta\omega = \omega_2 - \omega_1 \cong \frac{\omega_0}{Q_R} = 2\lambda \tag{21}$$

We have also to note that $S_{xx}(\omega=0) = 0$ (in contrast to model A). This feature seems to affect positively the fit of the background term. Furthermore, the transfer functions of models A and B have the same (conjugate complex) poles. The difference is that, in model A, the transfer function corresponds to an AR(2) model, while in model B the transfer function is related to an ARMA(2,1) model (in the backward difference approximation by the z-transform).

The ideal ACF follows from the inverse Fourier transform of Equation (18) and reads:

$$R_{xx}^{(I)}(\tau) = C_0 e^{-\lambda|\tau|}\left[\cos(\omega_c \tau) - \frac{\lambda}{\omega_c}\sin(\omega_c|\tau|) \right] \tag{22}$$

where ω_c has the value given by Equation (2). The relationship between A_0 and C_0 is that given by Equation (6). Equations (22) and (5) differ only in the negative sign of the second term. With respect to the minima and maxima of $R_{xx}^{(1)}(\tau)$, regarding only the right-hand side of the equation for $\tau > 0$, the extrema appear in model A (Equation (5)) exactly at multiples of τ/ω_c . In model B they occur at down-shifted values of the lag time, and are given by:

$$\tau_n^{(min)} = \frac{2(n-1)\pi + \eta}{\omega_c}; n = 1,... \tag{23}$$

$$\tau_n^{(max)} = \frac{(2n-1)\pi + \eta}{\omega_c}; n = 1,... \tag{24}$$

$$\text{where } \eta = 2\arccos\frac{1}{2Q_R} \tag{25}$$

The values of $\tau_n^{(min)}$ and $\tau_n^{(max)}$ do not deviate very much from those of model A, if DR > 0.2, and this suggests that the same definition of the DR can be used as given by Equation (7). Q_R is then related to the DR by:

$$Q_R = \frac{1}{2}\sqrt{1 + (\frac{2\pi}{\ln DR})^2} \tag{26}$$

In order to demonstrate some examples of these deviations numerically, we introduce lag-time shift factors defined by:

$$r_n^{(min)} = \tau_{n(model-B)}^{(min)} / \tau_{n(model-A)}^{(min)} = \frac{2(n-1)\pi + \eta}{(2n-1)\pi} \tag{27}$$

$$r_n^{(max)} = \tau_{n(model-B)}^{(max)} / \tau_{n(model-A)}^{(max)} = \frac{(2n-1)\pi + \eta}{2n\pi} \tag{28}$$

Results for the worst case (n = 1) are given in Table 1.

Table 1: $r_1^{(min)}$ and $r_1^{(max)}$ as Functions of the DR

DR	$r_1^{(min)}$	$r_1^{(max)}$
0.99	0.9990	0.9995
0.9	0.9893	0.9947
0.6	0.9484	0.9742
0.4	0.9078	0.9539
0.2	0.8404	0.9202

2.3 Signal Filter and Background Effects in the Fitting ACF (Numerical Examples)

Two FORTRAN codes were written in order to study the magnitude of the effects which perturb the

ideal ACF by signal filtering and inclusion of the PSD background. The code ACFOSC5 was written for model A, and the code ACFOSC6 for model B. The main input parameters, in both codes, are: ω_0 , DR, and sets of the 4 parameters (ω_L , ω_H , B_{0p}/P_{max}, S), so that several cases of signal filtering and background admixtures can be treated within a calculation. C_0 is set equal to 1. The IMSL routines DQDAWO and DQDAWF are used for performing numerical integration.

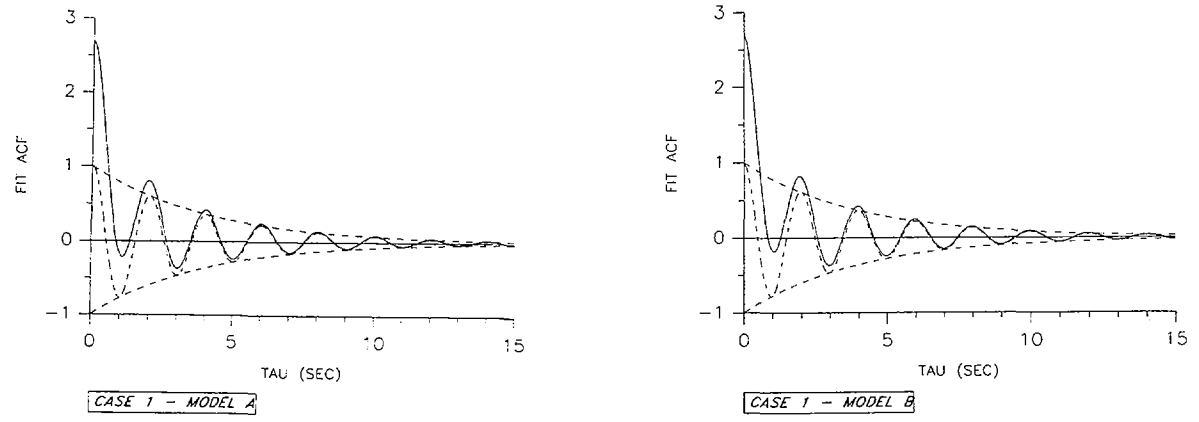

Fig. 1: Fitting ACFs (solid lines) – Model A and Model B
No Signal Filtering, PSD Background Admixture: B_{0p}/P_{max} = 10 %, S = -2
Ideal ACFs (dashed lines)

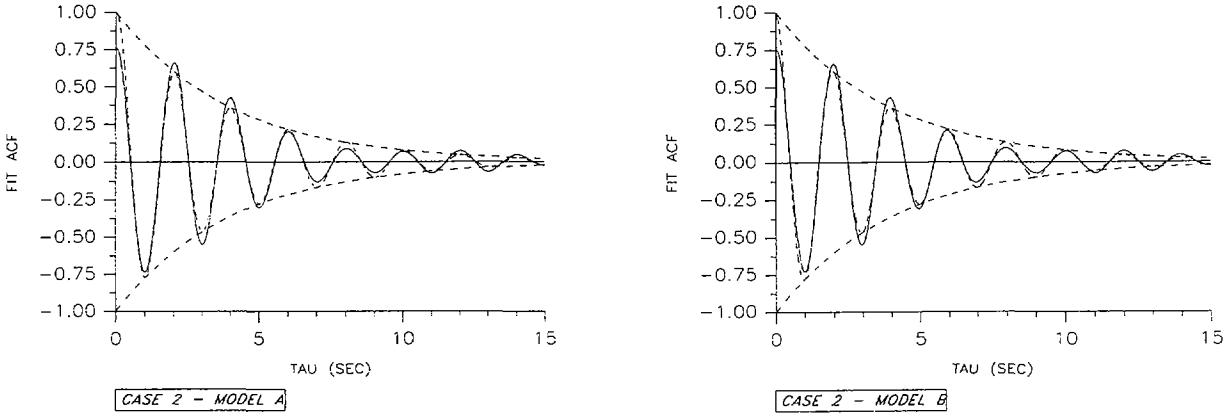

Fig. 2: Fitting ACFs (solid lines) – Model A and Model B
Strong Signal Filtering: 0.4 – 0.6 Hz, No PSD Background Admixture
Ideal ACFs (dashed lines)

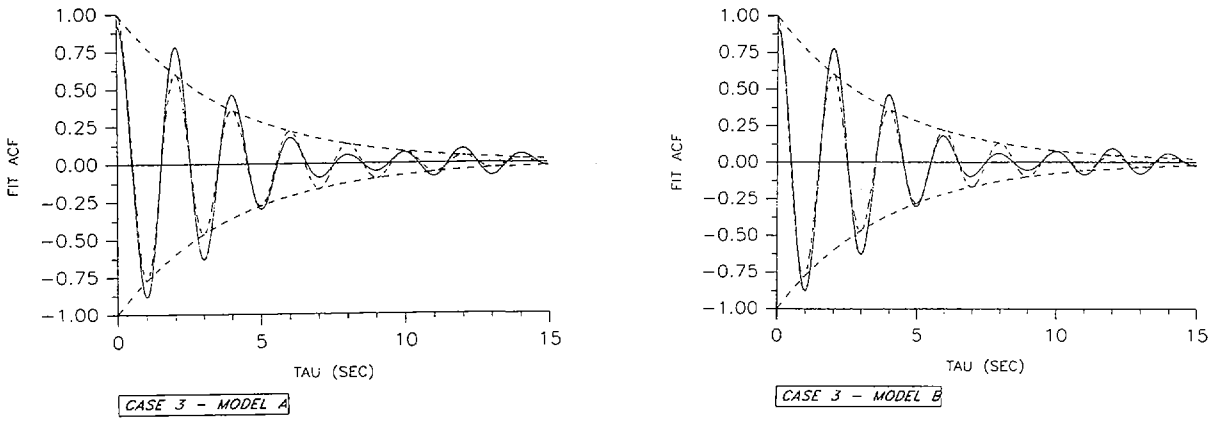

Fig. 3: Fitting ACFs (solid lines) – Model A and Model B
Strong Signal Filtering: 0.4 – 0.6 Hz
PSD Background Admixture: B_{0p}/P_{max} = 10 %, S = -2

Figs. 1 – 3 show three cases of the fitting ACFs for model A as well for model B, up to a lag time of 15 s. For each case, $\omega_c/2\pi$ = 0.5 Hz and DR = 0.6. The solid lines refer to the fitting ACFs, and the dashed lines to the ideal ACFs, with the envelopes for comparison.

In Case 1 (Fig. 1), no signal filtering is assumed, but there is a PSD background admixture with B_{0p}/P_{max} = 10 % and the slope index S = -2.

In Cases 2 and 3 (Figs. 2 and 3), very strong signal filtering is assumed, with $\omega_L/2\pi$ = 0.4 Hz and $\omega_H/2\pi$ = 0.6 Hz. Case 2 shows the fitting ACFs without the presence of background. In Case 3, background is admixed with the same data as in Case 1. A significant deformation of the ideal ACFs can be observed. It is obvious that this deformation decreases if one either widens the filter bandwidth or increases the DR. If one compares the two cases, the influence of background is significantly reduced with respect to Case 1.

Both models have practically identical fitting ACFs in the examples given. Appreciable differences appear, however, with decreasing DR values. Strange fitting ACF profiles can be produced, in particular with asymmetric filter cut-off frequencies. We primarily used model B in treating the benchmark signal data, because of the peak resonance frequency problem with model A.

3. Methods Applied to Signal Filtering and ACF Estimation

Our methods used for signal filtering and ACF estimation are both based on the application of fast Fourier transform (FFT) techniques with signal segmentation. Since most of the benchmark records are relatively short, containing about 4000 – 5000 data points, the selection of the segment length N_s of 256 data points was found to be a reasonable compromise between resolution and statistical requirements.

3.1 Signal Filtering with an FFT Filter

In principle, any digital filter type which has smooth characteristics and is very steep at the corner frequencies can be used for band-pass filtering of signal data. However, the simplest digital filter which approximates the shape of an ideal rectangular filter, as assumed in our oscillator models, is obtained by FFT techniques. We thus developed an interactive FORTRAN code, called FFTF2, for which the FFT routines were taken from IMSL. The data in a segment are initially Fourier

transformed. Depending to the given values for ω_L and ω_H , the code searches for the nearest possible values ω_{Lp} and ω_{Hp} which are multiples of the Nyquist co-interval. These values have then to be transferred as input parameters to our fitting codes. The (complex) spectral coefficients are retained in the possible closed frequency interval $[\omega_{Lp}, \omega_{Hp}]$, the other coefficients, outside this interval, are set equal zero. The inverse FFT then gives the filtered signal data in a segment. In this way, the data are treated segment by segment. One can also apply low-pass filtering alone. In this case, two options are available for DC component removal, either with a DC value calculated over all segments, or locally with DC values calculated for each segment separately. Our FFT filter is not universal and is not listed in the modern filter handbook by Chen (1995). It is related solely to our ACF estimation procedure. It picks out the frequency components at multiples of the Nyquist co-interval within the given cutoff frequencies and does not show any "Gibbs" phenomena after return to the time domain by the inverse Fourier transform. The latter is a disadvantageous feature of the usual nonrecursive digital filters. One may assume that the signal data before filtering exhibit the digital image of a continuous record, and hence the filtered data can be regarded as being continuous within a segment. However, discontinuities appear on the edges between succeeding segments. These lead to distortions in a PSD estimation using the same segment length, but with time-shifted scanning, i.e. if one starts scanning, for example, in the middle of the first segment.

3.2 ACF Estimation

In the direct ACF estimation procedure, an unbiased estimate, assuming N data samples, is obtained by:

$$\hat{R}_{xx}(n) = \frac{1}{N-n} \sum_{m=0}^{N-n-1} x(n)x(n+m); 0 \le n \le N-1 \tag{29}$$

It is worthwhile making an estimation over the entire available record length. Figure 4 shows an example of an ACF (covariance function, DC component removed) estimated on the unfiltered benchmark record C4_LPRM.8.

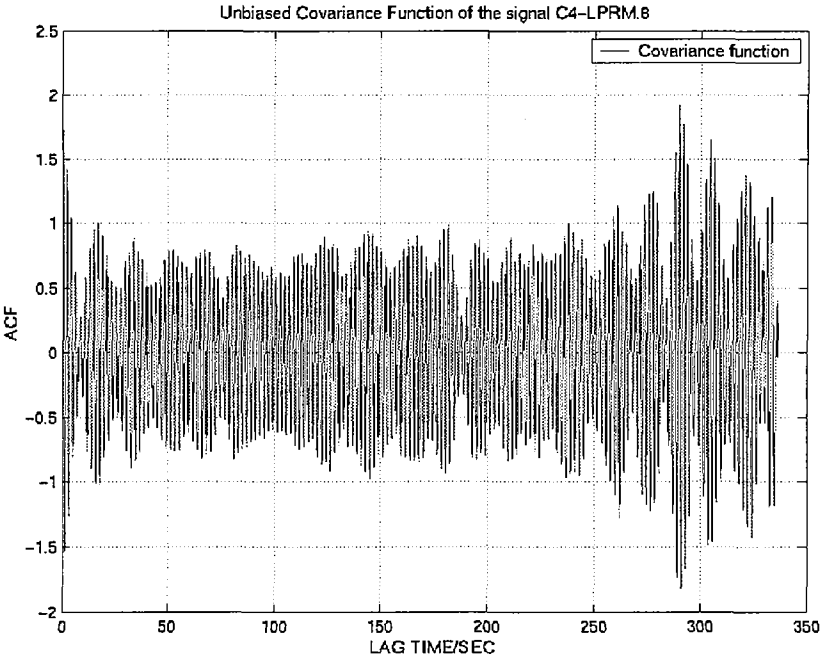

Fig. 4: Unbiased Covariance Function Estimate on the Unfiltered Benchmark Record C4_LPRM.8 over the Complete Record Length

A code available in MATLAB (1992) was used for this analysis. After the initially decaying oscillations, which are represented in Fig. 5, further oscillations appear which give the impression of beats if regions are plotted with higher resolution.

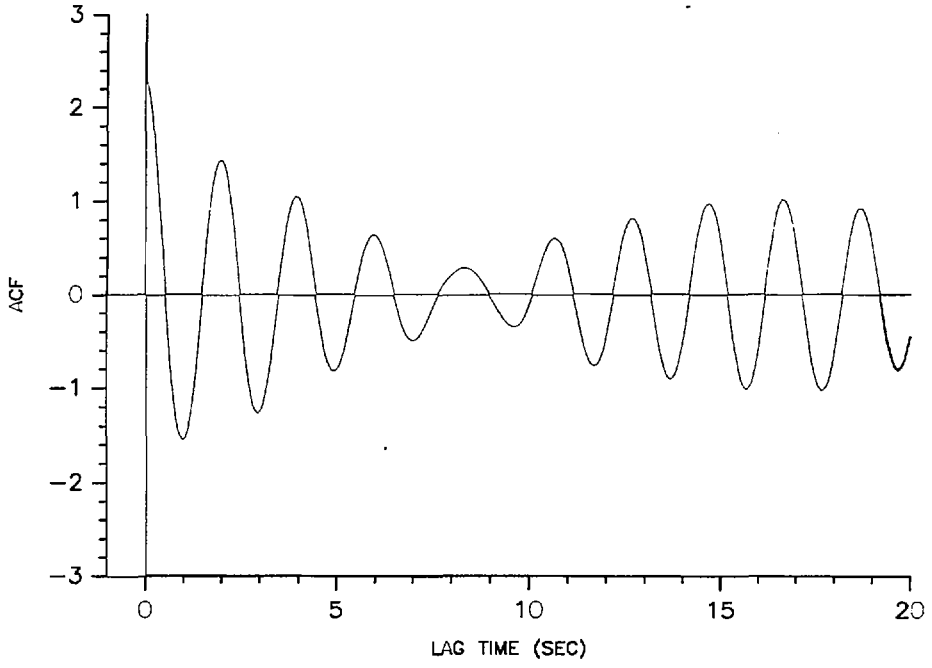

Fig. 5: Unbiased Covariance Function Estimate on the Unfiltered Benchmark Record C4_LPRM.8 Initial Part of Fig. 4, up to a Lag Time of 20 s.

It is obvious that the uncertainty of the estimate increases towards the end of the lag-time range. If a covariance function estimate is performed on the band-pass filtered signal, only a qualitative change results.

The ACF estimation procedure we have used here is based on the indirect and slightly modified method using FFT techniques and zero padding (Bendat and Piersol, 1971). The effective FFT transform size is $2N_s$. The method is especially suitable for picking out the interesting initial part of the ACF. Our bivariate code ACCF1, written and documented by Behringer (1988), can deliver ACF estimates (and also estimates of the cross-correlation function (CCF)) for selected single segments, which we call instantaneous ACFs, or ACF estimates for a given number N_{av} of successive segments. If N_{av} is very large, the code scans over all completely filled segments which are commonly available in both channels. In the later application, we speak briefly of average ACFs. However, such an average ACF is not simply an average of instantaneous ACFs. The calculated raw segment PSDs are averaged before the inverse FFT is applied for calculating the circular ACF estimate, from which the true ACF estimate follows by decomposition.

The application to our filtered signal data requires the use of the same segment length and exact scanning, segment by segment. For checking the combination of FFT filtering and ACF estimation, as an alternative we performed data filtering with the detrending method of Behringer (1998), which is based on spline techniques. The present code version requires a double application for band-pass filtering. This filter type is very suitable for filtering at frequencies which are very low with respect to the Nyquist cut-off frequency. Using a 9^{th} order spline approximation, the steepness at the corner frequency is of the order of –80 db per octave. Comparison of ACF estimates on some actual neutron signal data, filtered either by the FFT filter or by the spline filter, showed nearly identical results.

The code ACCF1 allows three different kinds of DR determination to be made :

(1) An average ACF can be estimated over all available segments, and a least-squares fit then performed. In this case, no information is obtained about the statistical uncertainty of the results.

(2) Instantaneous ACFs (with N_{av}=1) can be successively estimated and fitted, and the average DR value and its standard deviation calculated. We call this procedure a segment analysis (SA). With a segment length of 256 data points, 15 individual DR values were normally available. We looked particularly at signal cases where the process was essentially stationary. However, instantaneous ACF estimates in most cases showed very large scattering with often strange ACF shapes from segment to segment. It seldom happened that all instantaneous ACF estimates of a filtered signal record could be fitted. We had to leave out non-fittable ACFs in this kind of uncertainty analysis.

(3) A gliding segment analysis (GLSA) can be performed, which we have defined to be when 'short-term' ACFs are estimated with a low fixed value of N_{av} segments. The first ACF estimate is obtained from the signal data in the first N_{av} segments. Each following ACF estimate is based on taking the signal data in the succeeding segment and keeping the data in the N_{av}-1 previous segments. One obtains a set of (strongly correlated) ACFs which move with some averaging over the signal length, each forward shifted by one segment. If the signal contains N_{seg} segments, the number of ACF estimates is given by N_{seg}-N_{av}+1. We used N_{av}=5, and fits of these ACFs showed promising results, with significantly lower standard deviations of the average DR values than observed in the SA. The GLSA is moving in the direction of being an on-line procedure. In principle, a new DR value is available after about each 20 s. The modified code ACCF2 was used for the SA and GLSA procedures, which simplifies the parameter data input required for the code ACCF1.

4. Fitting Procedure

Considering only the right-hand side of the ACF (since an ACF is a symmetrical function of τ), the experimental ACF estimated by the code ACCF1 covers the lag-time range τ_{max}=20.48 s (N_s=256, sampling frequency 12.5 Hz). The ACF data point at the lag number N_s is undefined, but is set equal to zero in ACCF1. There are two reasons for keeping the fitting range variable within τ_{max} :

a) The statistical accuracy of an ACF estimate (either by the direct or the indirect method) decreases with increasing lag time values, simply because the number of signal data products involved in averaging decreases. In order to be on the safe side, the use of an ACF estimate should be restricted to about 50 % of τ_{max}. However, values of up to 70 % are acceptable.

b) Even in the case of strong signal filtering, all our ACF estimates showed the more or less significant appearance of 'short-term' ACF background after the decay of the main oscillation. A typical example is shown in Fig.5. The presence of this 'short-term' background suggests an individual adaptation of the fitting range to the DR value. In particular, cases with small DR values (which are of minor importance in BWR stability surveillance) can only be fitted over relatively short lag-time ranges. This, however, leads to large uncertainties in the results.

4.1 Fitting Codes

An experimental and highly modular FORTRAN code, called ACFIT, has been developed using double precision accuracy. A set of fitting-range parameters r (0<r<1) is given for each calculation run. The integer value of rN_s determines the last ACF data point to be included in the fit, and defines the lag-time end point, τ_{end} , for a fit. The r values are arranged in ascending order by the code. We will refer to a fit with a specified r value as a *job* within a run. The other important input parameters are: ω_L and ω_H (their values needing to be transferred from the code FFTF2 in filtered-signal cases), the option parameter IBGR with respect to the PSD background treatment in the models (Section 2.1), the option parameter IWEIGHT for selecting one of the six functions provided for weighting the squared errors in a fit (to be explained later), and initialisation values for the fitting parameters B_0 and α, if IBGR>0. The value to be given for B_0 is not critical, since B_0 enters linearly in the model ACF. It is input by the value b_0 (>0), so that $B_0 = b_0 \hat{R}_{xx}(\tau = 0)$. The slope index S (Equation (14)) is used instead of α, and the initial value of α is then internally calculated. The values of the main fitting parameters C_0, ω_c and λ are initialised by the code: $C_0 = \hat{R}_{xx}(\tau = 0), \omega_c / 2\pi = 0.5$ Hz, for the cases of unfiltered or weakly filtered signal cases (or $\omega_c = (\omega_L + \omega_H)/2$ otherwise), and λ from a DR=0.6. The initialised fitting parameter values refer to the start of the first job (smallest value of τ_{end}). They are stored as a basic set, to which a reset can be made. Under normal run conditions, each following job starts with the fitting parameter values estimated from the preceding job. The code takes countermeasures if the following anomalous conditions occur :

a) A job is allowed to repeat itself once with a complete fitting parameter reset, if C_0<0 or if λ<-0.1 result, or the fit does not converge. A negative value of C_0 can appear in cases with strongly filtered signal data. Such a fit is, however, worthless. A negative value of λ violates the models, but a small negative value must be allowed considering data scatter in cases with high DR values (limit cycle cases). The evaluations of P_{max} (Equation (15)) and B_{0p} (Equation (16)) are restricted to DR<1 and $\hat{\omega}_r > \omega_L$. Otherwise these values are set to zero. Obviously, job repetition is only allowed if the job in question did not begin with the basic set of fitting parameter values. A job with a 'bad' or non-converging fit is cancelled and the code continues with the next job, with a complete fitting parameter reset.

b) A fit is interrupted if ω_r becomes imaginary (model A) or α drops below a given negative level. The latter can otherwise lead to overflow conditions. The job in question is cancelled and the code continues with the next job, with a complete fitting parameter reset.

c) The next job also starts with a complete fitting parameter reset, if, in the preceding job, a $\hat{DR} < 0.2$ has been estimated.

d) A partial reset is provided for the next job, with the starting conditions λ=0, if $-0.1 \le \hat{\lambda} < 0$, or with the basic values of B_0 and α (IBGR=2) if $\hat{B}_0 < 0$ or $\hat{\alpha} \ge 10$ in the preceding job. The appearance of small negative values of B_0 must be permitted, because of data scatter.

All the fitting parameter data of the jobs and, in addition, the derived data $\hat{A}_0, \hat{DR}, \hat{P}_{max}$ and the reduced chi-square χ^2_R (the sum of the weighted squares divided by the number of degrees of freedom) are written to a file where the data of cancelled jobs are set equal to 10^{30} and can be recognised. In the SA and GLSA, the auxiliary code ACFITEV5 handles the data matrices from the

different runs and calculates averages and standard deviations of each variable for each job, with cancelled jobs being eliminated. Hence, these average data and standard deviations refer only to the number of 'good' ACFs for each job separately.

Several versions of our fitting code exist. The current final versions are: ACFIT6 for model A, and ACFIT7 for model B. One might believe that least-squares fitting is today a rather trivial procedure. This is not so in the present application. Originally, we started with the IMSL non-linear regression routine DRNLIN, which was used with both options, to obtain the gradient of the fitting function either by finite differences (IDERIV=0) or by supplied gradient functions (IDERIV=1). The numerical integrations involved in our models (using the IMSL routines DQDAWO and DQDAWF) required a parameter setting for a high precision which, for guaranteeing convergence, indicated that the integration interval $(0,\omega_L)$ be divided into the two subintervals $(0,\omega_r)$ and (ω_r,ω_L), if (instantaneous) values of ω_r lay below ω_L during a fit, and correspondingly for the interval (ω_H,∞). Even with these provisions, many fits did not converge, indicating numerical instabilities. Since it is not easy to adapt this fitting routine to non-default convergence criteria, we replaced it by the old routine MARFIT, developed and documented by Behringer (1970). MARFIT is based on a combination of the Gauss-Newton method with a modified version of the gradient-expansion method by Marquardt (1963). This routine is very flexible in its application. All convergence criteria must be given separately in the calling routine. The criteria used here were simply based on minimising χ^2_R under the constraint of a prescribed smallness of the gradient-expansion coefficient. Stronger additional convergence criteria for each single fitting parameter were not included. MARFIT allows computational optimisation for avoiding calculation repetition of parts of the fitting function which appear in the gradient functions.

The six available functions introduced for weighting the square errors in the fit are of the type:

$$w(\tau) = w_1(\tau)w_0(\tau) \tag{30}$$

For the values of the option parameter IWEIGHT=1-3, $w_1(\tau) = 1$. $w_0(\tau)$ is given for:

IWEIGHT=1: $w_0(\tau) = 1$ (uniform weighting) (31)

IWEIGHT=2: $w_0(\tau) = 1 - \tau/\tau_{end}$ (linearly decreasing weighting) (32)

IWEIGHT=3: $w_0(\tau) = \cos(\pi\tau/2\tau_{end})$ (cosine-shaped weighting) (33)

$$0 \le \tau \le \tau_{end}$$

For IWEIGHT=4-6, $w_0(\tau)$ corresponds to the functions selected by IWEIGHT=1–3. $w_1(\tau)$ permits an initial reduction of weighting, and has the form:

$$w_1(\tau) = w_a + (1-w_a)\sin(\pi\tau/2\tau_a); 0 \le \tau < \tau_a << \tau_{end}, 0 \le w_a < 1$$
$$= 1; \tau \ge \tau_a \tag{34}$$

w_a and τ_a are additional input parameters. The weighting function of interest has been found for IWEIGHT=3. There is a further option parameter for stretching out $w_0(\tau)$ of Equations (32) or (33) by replacing τ_{end} by τ_{max}. We only made use of this option at the beginning of our investigations, when τ_{end} exceeds 50 % of τ_{max}.

4.2 Fitting Sensitivity Studies

One may roughly divide the experimental ACFs into the three classes: low DR values (DR≤0.5); medium DR values (0.5<DR<0.8); and high DR values (DR≥0.8).

Artificially generated ACFs were used for testing the fitting codes (source code ACFOSC5 and fitting code ACFIT6 for model A; source code ACFOSC6 and fitting code ACFIT7 for model B). In this test procedure, almost all of the available fitting range (r≈90 %) must be applied.

The fitting sensitivity to the information loss involved in the variation of the fitting range and the filter bandwidth in the presence of the PSD background has been studied separately. Fixed parameter data in the source codes were:

$C_0 = 1$

$\omega_0 / 2\pi$ = 0.5 Hz

Sampling frequency 12.5 Hz

Segment length (assumed for lag time resolution) N_s = 256 data points

Varied input parameter data in the source and fitting codes were :

DR = 0.3, 0.5, 0.7, 0.9

Filter bandwidth (assumed to be symmetrical around ω_0): 0.4-0.6, 0.3-0.7, 0.2-0.8 Hz

Background slope index S = -0.5, -1.0, -1.5

Fitting range r = 15-50 % in steps of 2.5 % (15 jobs within one run of the fitting codes)

A constant background ratio $B_{0p} / P_{max} = 10$ % (Equations (15) and(16)) was assumed in the first stage of each investigation, carried out for both models with the fitting options IBGR=1,2 and 3, and IWEIGHT=1 and 3. Results can be summarised as follows:

1) The three-parameter fitting option IBGR=0, which neglects the background term in the fitting function, overestimates C_0 and underestimates the DR with a (in general slight) reduction of the oscillation frequency ω_c. There is practically no difference in the results if the weight function IWEIGHT=1 or IWEIGHT=3 are used in the fit. In order to demonstrate the orders of magnitude, Table 2 contains the numerical results for C_0, $\omega_c / 2\pi$ and DR obtained from model B with IWEIGHT=3, in the three fitting ranges r=15, 30 and 45 %.The estimated DR values which are nearest to the given values are obtained with the smallest filter bandwidth (0.4-0.6 Hz) and the slope index S=-0.5. Decreasing S values make the exponentially decaying PSD background under the peak steeper and increase B_0 (Equation (16)). If the filter bandwidth is increased, the background is more effective and the estimated DR values are further reduced. In the worst case, given in the last column in Table 2, the background becomes so dominant that this fitting option fails.

Table 2: Sensitivity Studies, Model B, IBGR=0, IWEIGHT=3, Part 1 : B_{0p}/P_{max} = 10 %

Source Parameter Values			Fit Range r = 15 %			Fit Parameter Values Fit Range r = 30 %			Fit Range = 45 %		
Filter-Width (Hz)	f_c (Hz)	Slope Index	C_0	f_c (Hz)	DR	C_0	f_c (Hz)	DR	C_0	f_c (Hz)	DR
DR=0.3											
0.4-0.6	0.4911	-0.5	1.1878	0.4921	0.2686	1.1859	0.4920	0.2695	1.1833	0.4920	0.2707
		-1.0	1.1852	0.4909	0.2693	1.1835	0.4909	0.2701	1.1811	0.4909	0.2712
		-1.5	1.1844	0.4898	0.2694	1.1829	0.4898	0.2702	1.1807	0.4899	0.2711
0.3-0.7		-0.5	1.2449	0.4938	0.2407	1.2310	0.4930	0.2493	1.2271	0.4928	0.2518
		-1.0	1.2489	0.4905	0.2386	1.2362	0.4906	0.2466	1.2330	0.4907	0.2489
		-1.5	1.2591	0.4874	0.2342	1.2471	0.4883	0.2418	1.2445	0.4885	0.2438
0.2-0.8		-0.5	1.2916	0.4956	0.2141	1.2711	0.4939	0.2304	1.2669	0.4935	0.2339
		-1.0	1.3097	0.4902	0.2043	1.2909	0.4906	0.2207	1.2872	0.4906	0.2243
		-1.5	1.3437	0.4848	0.1886	1.3251	0.4873	0.2056	1.3218	0.4876	0.2093
DR=0.5											
0.4-0.6	0.4970	-0.5	1.2518	0.4944	0.4422	1.2471	0.4947	0.4451	1.2399	0.4950	0.4491
		-1.0	1.2534	0.4934	0.4408	1.2488	0.4938	0.4438	1.2415	0.4941	0.4478
		-1.5	1.2567	0.4923	0.4388	1.2522	0.4928	0.4418	1.2448	0.4934	0.4460
0.3-0.7		-0.5	1.4064	0.4864	0.3534	1.3567	0.4911	0.3890	1.3309	0.4927	0.4070
		-1.0	1.4183	0.4822	0.3451	1.3655	0.4887	0.3820	1.3372	0.4910	0.4029
		-1.5	1.4406	0.4775	0.3327	1.3834	0.4860	0.3735	1.3514	0.4891	0.3955
0.2-0.8		-0.5	1.5489	0.4752	0.2678	1.4253	0.4889	0.3562	1.3900	0.4914	0.3807
		-1.0	1.5874	0.4654	0.2452	1.4401	0.4856	0.3472	1.4000	0.4891	0.3747
		-1.5	1.6632	0.4522	0.2095	1.4781	0.4812	0.3278	1.4283	0.4861	0.3607
DR=0.7											
0.4-0.6	0.4992	-0.5	1.3987	0.4962	0.5923	1.3862	0.4967	0.6005	1.3656	0.4973	0.6120
		-1.0	1.4012	0.4951	0.5907	1.3889	0.4956	0.5989	1.3681	0.4966	0.6107
		-1.5	1.4061	0.4939	0.5884	1.3939	0.4948	0.5966	1.3728	0.4959	0.6086
0.3-0.7		-0.5	1.7196	0.4847	0.4160	1.5990	0.4927	0.4957	1.5150	0.4957	0.5491
		-1.0	1.7399	0.4791	0.4052	1.6139	0.4902	0.4877	1.5227	0.4944	0.5452
		-1.5	1.7782	0.4728	0.3885	1.6445	0.4872	0.4734	1.5416	0.4929	0.5369
0.2-0.8		-0.5	2.0154	0.4672	0.2675	1.7185	0.4906	0.4450	1.6048	0.4947	0.5139
		-1.0	2.0919	0.4525	0.2352	1.7438	0.4871	0.4326	1.6171	0.4951	0.5082
		-1.5	2.2402	0.4321	0.1867	1.8114	0.4822	0.4034	1.6546	0.4987	0.4928
DR=0.9											
0.4-0.6	0.4999	-0.5	2.2376	0.4938	0.6089	2.1789	0.4950	0.6336	2.0813	0.4965	0.6700
		-1.0	2.2429	0.4915	0.6076	2.1864	0.4933	0.6316	2.0895	0.4953	0.6677
		-1.5	2.2551	0.4892	0.6054	2.2009	0.4914	0.6283	2.1047	0.4940	0.6638
0.3-0.7		-0.5	3.5413	0.4656	0.2605	3.0936	0.4829	0.3822	2.7162	0.4921	0.5035
		-1.0	3.5881	0.4531	0.2527	3.1820	0.4755	0.3604	2.7734	0.4888	0.4879
		-1.5	3.6940	0.4398	0.2415	3.3584	0.4656	0.3233	2.9139	0.4839	0.4528
0.2-0.8		-0.5	4.8565	0.4091	0.0742	3.9991	0.4644	0.2080	3.3129	0.4857	0.3684
		-1.0	5.0699	0.3715	0.0563	4.9797	0.4047	0.0711	3.6773	0.4721	0.2847
		-1.5	5.4725	0.3287	0.0395	6.700	0.2247	0.0012	7.0243	0.1734	0.0001

2) The four-parameter fitting option IBGR=1 is problematic. Despite the fact that exactly the same slope index values are given as input to the fitting codes as to the source codes, at small fitting-range values a significant underestimation of the DR can be observed. Also, significant overestimation can occur. However, the fitting parameter data tend to approach (often weakly oscillating) the correct values with increasing fitting range values. This fitting option requires fitting ranges exceeding 50 % of τ_{max}. The behaviour in small fitting ranges may be explained by the competition between the linearly entering fitting parameters C_0 and B_0. At the beginning of our method development, we applied this fitting procedure to the average ACF of several benchmark records, and obtained often apparently reasonable results, where the plots of the average ACF and the fit ACF showed very good agreement. The GLSA, however, would require the input of an individual slope index value for each short-term ACF. If one uses only a common S value taken approximately from the PSD estimated over the entire record length, the GLSA fails. Individual S values are not obtainable. The data of PSD estimations over 5 segments have too much scatter. We have therefore rejected this fitting option.

3) The five-parameter fitting option IBGR=2 exhibits the following features, which are best regarded as functions of the DR:

   a) For the low DR cases (DR=0.3 and 0.5), the filter bandwidth 0.4-0.6 Hz seems to be the minimum requirement for good fits, characterised by agreement of the fitting parameter data and the source parameter data, to the three significant digits. Good fits start at a fitting range of about r = 20 %. Larger filter bandwidths (0.3-0.7, 0.2-0.8 Hz) lead in general to good fits, starting with the given lower limit of r = 15 %.

   b) The medium DR case (DR=0.7) exhibits the trend that good fits require a higher fitting range of at least r = 25 %, with the weight function IWEIGHT=1. This value is shifted slightly upward if using the weight function IWEIGHT=3.

   c) These trends continue with the high DR case (DR=0.9), but good fitting results are no longer obtainable with the smallest filter bandwidth (0.4-0.6 Hz). Here the information deficit is too large to enable a difference to be distinguished between $R_{xx}^{(C)}(\tau)$ and $B(\tau)$.

The assumption of B_{0p} / P_{max} = Constant for the selected DR cases is unrealistic with respect to the observed PSDs. However, it has deliberately been chosen in order to study the trends of the fitting sensitivity. In the second part of our investigations, which were made with only model B, the fitting options IBGR=1 and 3 and IWEIGHT=3, calculations were repeated with the assumption B_{0p} = Constant. The value of B_{0p} was taken from B_{0p} / P_{max} = 20 %, for DR=0.3. For the three-parameter fitting option IBGR=0, Table 3 gives the numerical results for C_0, $\omega_c / 2\pi$ and DR, in the same way as shown previously in Table 2. The five-parameter fitting option IBGR=2 exhibited the same trends as previously commented on in the first part of the investigations. Since, in the high DR case (DR=0.9), the PSD background is relatively small, the ACFs generated with the filter bandwidth 0.4-0.6 Hz allowed good fits, which started at about r = 30 %.

Table 3: Sensitivity Studies, Model B, IBGR=0, IWEIGHT=3, Part 2 : B_{0p} = constant

Source Parameter Values			Fit Parameter Values Fit Range r = 15 %			Fit Range r = 30 %			Fit Range = 45 %		
Filter-Width (Hz)	f_c (Hz)	Slope Index	C_0	f_c (Hz)	DR	C_0	f_c (Hz)	DR	C_0	f_c (Hz)	DR
DR = 0.3 B_{0p}/P_{max} = 20 %											
0.4-0.6	0.4911	-0.5	1.3991	0.4847	0.2381	1.3955	0.4850	0.2396	1.3903	0.4853	0.2415
		-1.0	1.3994	0.4822	0.2365	1.3961	0.4827	0.2379	1.3912	0.4831	0.2398
		-1.5	1.4035	0.4796	0.2341	1.4005	0.4802	0.2355	1.3960	0.4807	0.2373
0.3-0.7		-0.5	1.5738	0.4719	0.1741	1.5355	0.4764	0.1904	1.5263	0.4776	0.1946
		-1.0	1.5874	0.4643	0.1664	1.5512	0.4703	0.1822	1.5431	0.4718	0.1861
		-1.5	1.6169	0.4556	0.1556	1.5842	0.4630	0.1698	1.5788	0.4648	0.1727
0.2-0.8		-0.5	1.7588	0.4512	0.1110	1.6658	0.4664	0.1473	1.6470	0.4692	0.1553
		-1.0	1.8121	0.4327	0.0923	1.7175	0.4534	0.1269	1.6955	0.4574	0.1356
		-1.5	1.9162	0.4076	0.0676	1.8443	0.4312	0.0902	1.8231	0.4364	0.0972
DR = 0.5 B_{0p}/P_{max} = 11.65 %											
0.4-0.6	0.4970	-0.5	1.2951	0.4940	0.4338	1.2896	0.4943	0.4371	1.2812	0.4946	0.4415
		-1.0	1.2968	0.4928	0.4323	1.2915	0.4932	0.4356	1.2831	0.4937	0.4401
		-1.5	1.3007	0.4916	0.4301	1.2954	0.4922	0.4335	1.2869	0.4928	0.4381
0.3-0.7		-0.5	1.4777	0.4848	0.3352	1.4203	0.4900	0.3735	1.3909	0.4919	0.3928
		-1.0	1.4914	0.4799	0.3263	1.4311	0.4872	0.3667	1.3990	0.4899	0.3878
		-1.5	1.5174	0.4745	0.3131	1.4533	0.4840	0.3554	1.4172	0.4875	0.3788
0.2-0.8		-0.5	1.6485	0.4714	0.2422	1.5054	0.4872	0.3350	1.4643	0.4901	0.3616
		-1.0	1.6951	0.4597	0.2179	1.5254	0.4831	0.3236	1.4781	0.4872	0.3538
		-1.5	1.7865	0.4439	0.1805	1.5772	0.4772	0.2990	1.5169	0.4833	0.3356
DR = 0.7 B_{0p}/P_{max} = 6.023 %											
0.4-0.6	0.4992	-0.5	1.2351	0.4973	0.6305	1.2277	0.4977	0.6362	1.2154	0.4981	0.6442
		-1.0	1.2368	0.4966	0.6294	1.2294	0.4971	0.6352	1.2158	0.4977	0.6434
		-1.5	1.2399	0.4959	0.6276	1.2324	0.4965	0.6336	1.2195	0.4972	0.6421
0.3-0.7		-0.5	1.4187	0.4902	0.5037	1.3447	0.4955	0.5673	1.2931	0.4973	0.6070
		-1.0	1.4309	0.4867	0.4949	1.3515	0.4942	0.5629	1.2962	0.4966	0.6053
		-1.5	1.4534	0.4828	0.4811	1.3659	0.4927	0.5547	1.3041	0.4959	0.6014
0.2-0.8		-0.5	1.5783	0.4807	0.3870	1.4002	0.4947	0.5389	1.3352	0.4969	0.5882
		-1.0	1.6177	0.4726	0.3611	1,4089	0.4931	0.5337	1.3394	0.4961	0.5861
		-1.5	1.6957	0.4616	0.3177	1.4330	0.4912	0.5210	1.3534	0.4952	0.5796
DR = 0.9 B_{0p}/P_{max} = 1.782 %											
0.4-0.6	0.4999	-0.5	1.1974	0.4986	0.8259	1.1879	0.4990	0.8349	1.1707	0.4994	0.8475
		-1.0	1.1988	0.4981	0.8251	1.1892	0.4986	0.8342	1.1717	0.4992	0.8471
		-1.5	1.2013	0.4976	0.8237	1.1915	0.4983	0.8330	1.1735	0.4990	0.8462
0.3-0.7		-0.5	1.3783	0.4929	0.6752	1.2892	0.4978	0.7661	1.2178	0.4992	0.8244
		-1.0	1.3891	0.4902	0.6672	1.2937	0.4972	0.7633	1.2191	0.4989	0.8239
		-1.5	1.4088	0.4872	0.6534	1.3033	0.4964	0.7573	1.2228	0.4987	0.8222
0.2-0.8		-0.5	1.5288	0.4856	0.5384	1.3231	0.4976	0.7478	1.2403	0.4991	0.8144
		-1.0	1.5628	0.4796	0.5125	1.3279	0.4969	0.7453	1.2421	0.4989	0.8137
		-1.5	1.6300	0.4716	0.4663	1.3416	0.4960	0.7377	1.2485	0.4986	0.8110

5. Analysis of Benchmark Data and Discussions

From the 91 benchmark records, we arbitrarily selected 19 signals which were measured under nearly stable reactor conditions and belong to low, medium and high DR cases. We give here only analysis results obtained by the GLSA with model B, as model B is superior to model A. For very low DR cases, we have not observed that the peak resonance frequency, ω_r , appears below ω_c in estimated PSDs. The code ACFIT7SA was written in order to automate the GLSA, with the code ACFIT7 incorporated as a subroutine. The files with the ACF data generated by the code ACCF2 are successively called in the main program. The fitting range r was covered from 15 to 50 % in steps of 2.5 %. In low DR cases, and visible from PSD plots, the upper boundary of r was for the most part somewhat reduced.

5.1 Criterion for the Optimum Fitting Range

The most crucial question is that concerning the optimum fitting range. We found empirically that the standard deviation of the DR as a function of r or τ_{end} — $s_{DR}(r)$ or $s_{DR}(\tau_{end})$, respectively — passes through a minimum. This minimum (which is subjected to statistical scattering) is often not very sharp. It lies mostly towards the lower boundary of r in low DR cases, or, vice-versa, towards the upper boundary of r at high DR. This behaviour corresponds to the requirements found in the fitting sensitivity studies (Section 4.2) for the fitting option IBGR=2. Here we use this criterion for selecting the 'best' fits with the weighting function IWEIGHT=3. The use of this weighting function gives, in general, smoother curves for $\overline{DR}(r)$ and $s_{DR}(r)$ than the use of the weighting function IWEIGHT=1 would give. An example of this is given in Fig.6 for the three-parameter fitting procedure:

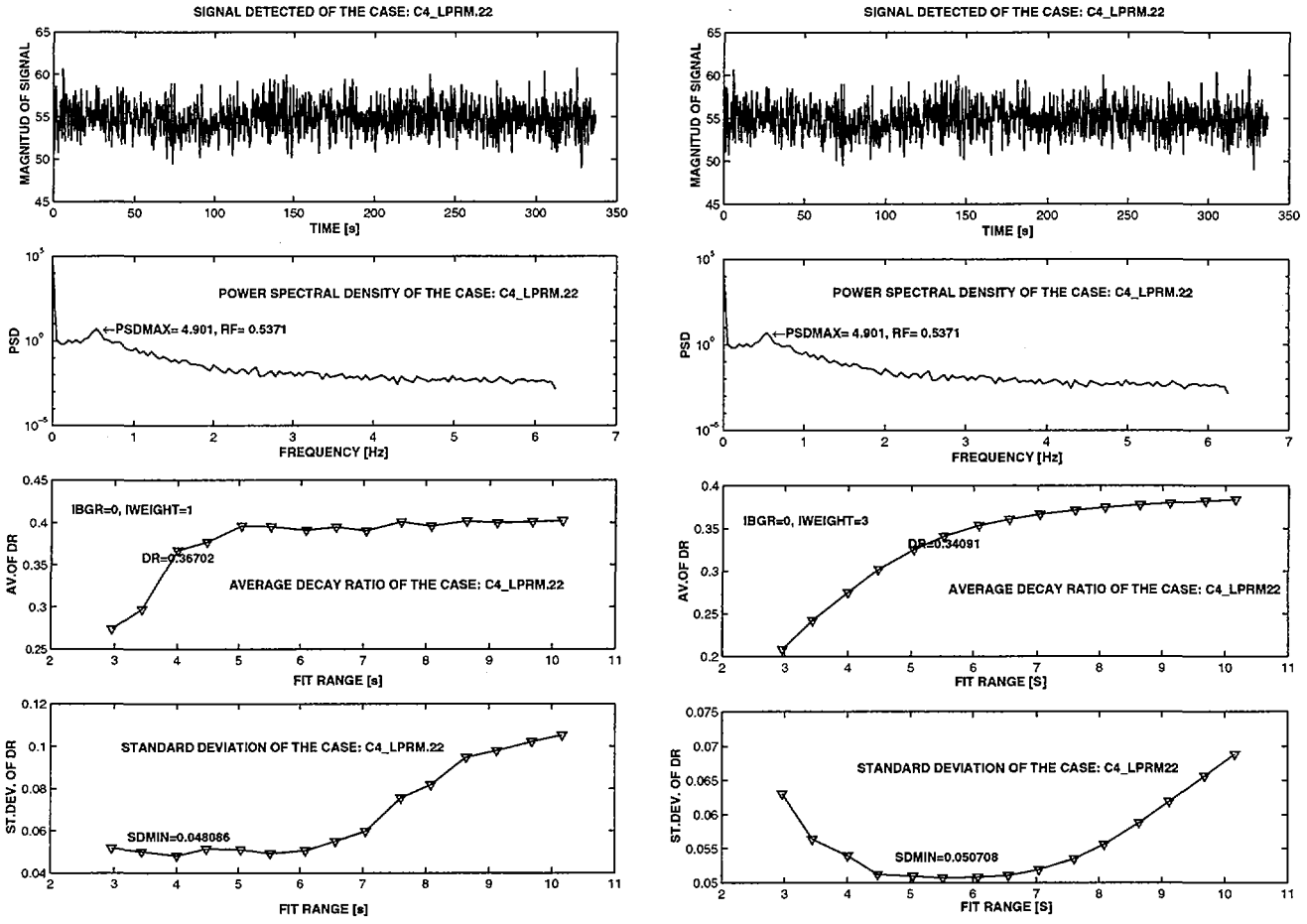

Fig. 6: Time Series, Power Spectral Density, Average Decay Ratio vs Fit Range and its Standard Deviation vs Fit Range (subplots 1-4) of the filtered Signal C4_LPRM.22 (Table 4)
Left Fig. : Fitting Procedure with IBGR=0, IWEIGHT=1)
Right Fig.: Fitting Procedure with IBGR=0, IWEIGHT=3

Some studies with the weighting function IWEIGHT>3 did not show any improvements. The quantity $\overline{\chi_R^2}$ as a function of r is not suitable for establishing a further criterion for the optimum fitting range. In general, this quantity increases initially, and can then develop into a plateau or decrease. However, its standard deviation $s_{\chi_R^2}(r)$ is of the same order of magnitude as $\overline{\chi_R^2}(r)$. A useful quantity is $\overline{P}_{max}$ (together with its standard deviation), which can be compared (for reasons of consistency) with the peak amplitude in the PSD estimation at low and medium DR cases at the 'best' fits. We mostly observed very good agreement within statistical accuracy (fitting option IBGR=2). It is obvious that the optimum fitting range must not coincide between the three-parameter and the five-parameter fitting procedure on the same ACFs. Five-parameter fits, where $|B_0|$ and α run to large values, have been accepted.

5.2 Numerical Results

In Table 4 we summarise the numerical results of the benchmark records analysed. Each record has been treated with the three-parameter and the five-parameter fitting procedures.

Table 4: Results for the Oscillation Frequency and the Decay Ratio

I	Record	Filter Bandwidth (Hz)	IBGR	No. of ACFs g	a	Fit Range r (%)	tau-end (s)	Frequency f (Hz)	s	Decay Ratio DR	s
1	C1_APRM.1	0.2441-0.7813	0	11	11	15.0	2.96	0.397	0.014	0.355	0.051
			2	11	11	15.0	2.96	0.438	0.009	0.598	0.055
2	C1_APRM.3	0.2930-0.7813	0	11	11	15.0	2.96	0.429	0.018	0.323	0.094
			2	11	11	27.5	5.52	0.479	0.020	0.603	0.094
3	C1_APRM.4	0.3418-0.6348	0	11	11	15.0	2.96	0.457	0.014	0.409	0.077
			2	11	11	22.5	4.48	0.486	0.012	0.698	0.170
4	C1_APRM.12	0.3418-0.6348	0	11	11	17.5	3.44	0.438	0.016	0.645	0.107
			2	11	11	40.0	8.08	0.466	0.004	0.822	0.039
5	C2_TEST.S11	0.1465-0.6836	0	11	11	15.0	2.96	0.309	0.023	0.101	0.072
			2	11	11	15.0	2.96	0.382	0.031	0.308	0.071
6	C2_TEST.S31	0.2930-0.6836	0	11	11	17.5	3.44	0.385	0.016	0.277	0.080
			2	11	11	27.5	5.52	0.433	0.016	0.490	0.061
7	C2_TEST.L1	0.2441-0.7813									
	Block 1		0	18	18	35.0	7.04	0.346	0.037	0.189	0.104
			2	18	13	25.0	5.04	0.408	0.027	0.384	0.084
	Block 2		0	18	18	15.0	2.96	0.374	0.022	0.286	0.086
			2	18	18	17.5	3.44	0.422	0.016	0.481	0.039
	Block 3		0	14	14	20.0	4.00	0.364	0.022	0.237	0.039
			2	14	14	15.0	2.96	0.414	0.011	0.458	0.061
	Total		0	50	50	20.0	4.00	0.366	0.024	0.254	0.086
			2	50	49	17.5	3.44	0.411	0.022	0.443	0.086
8	C2_TEST.L2	0.2441-0.7813									
	Block 1		0	18	18	17.5	3.44	0.483	0.015	0.397	0.076
			2	18	12	22.5	4.48	0.509	0.012	0.621	0.072
	Block 2		0	18	18	15.0	2.96	0.457	0.023	0.324	0.106
			2	18	18	15.0	2.96	0.502	0.007	0.636	0.065
	Block 3		0	14	14	27.5	5.52	0.479	0.007	0.413	0.078
			2	14	10	22.5	4.48	0.494	0.009	0.565	0.027
	Total		0	50	50	15.0	2.96	0.464	0.020	0.348	0.092
			2	50	50	20.0	4.00	0.504	0.012	0.629	0.073
9	C4_LPRM.8	0.3418-0.7324	0	12	12	32.5	6.56	0.502	0.005	0.716	0.035
			2	12	8	15.0	2.96	0.502	0.005	0.747	0.021
10	C4_LPRM.22	0.3418-0.7324	0	12	12	27.0	5.50	0.502	0.014	0.340	0.051
			2	12	12	35.0	7.04	0.517	0.015	0.609	0.066
11	C6_LPRM.111	0.2441-0.8789	0	12	12	15.0	2.96	0.357	0.040	0.067	0.044
			2	12	10	15.0	2.96	0.421	0.023	0.180	0.075
12	C6_LPRM.112	0.2441-0.8301	0	12	9	15.0	2.96	0.262	0.099	0.020	0.014
			2	12	12	15.0	2.96	0.459	0.019	0.270	0.063
13	C6_LPRM.22	0.2441-0.7813	0	12	12	15.0	2.96	0.383	0.032	0.057	0.038
			2	12	12	15.0	2.96	0.461	0.025	0.226	0.078
14	C6_LPRM.210	0.2441-0.7813	0	12	12	15.0	2.96	0.416	0.016	0.203	0.048
			2	12	12	15.0	2.96	0.476	0.008	0.512	0.087
15	C6_LPRM.211	0.4395-0.6836	0	12	12	50.0	10.16	0.523	0.001	0.947	0.016

16	C6_LPRM.213	0.3448-0.7324	0	12	12	50.0	10.16	0.523	0.001	0.960	0.013
			2	12	12	50.0	10.16	0.523	0.001	1.012	0.012
17	C6_LPRM.214	0.4395-0.6836	0	12	12	50.0	10.16	0.524	0.001	0.954	0.012
			2	12	12	50.0	10.16	0.525	0.001	1.005	0.026
18	C6_LPRM.215	0.3448-0.7324	0	12	12	50.0	10.16	0.523	0.001	0.981	0.006
			2	12	12	50.0	10.16	0.523	0.001	0.999	0.007
19	C6_LPRM.218	0.3906-0.6836	0	12	12	32.5	6.56	0.508	0.010	0.549	0.094
			2	12	12	32.5	6.56	0.517	0.009	0.745	0.200

Column 1 contains the current analysis number, I. The file name of the benchmark record is given in column 2. The applied filter bandwidth (with strong filtering) follows in column 3, having been somewhat subjectively taken from the previously estimated PSD with respect to the GLSA with IBGR=2. In particular, the lower filter cut-off frequency was chosen as the smallest value, to ensure the approximate validity of the assumed PSD background function, $B(\omega)$ (Equation (12)). Weak filtering, in general, gave either useless results or the fitting procedure failed. The fitting option value is given in column 4. In column 5, two values for the number of ACFs involved in the GLSA are listed. The first value denoted by 'g' refers to the given number of ACFs, the second value (denoted by 'a') is the accepted number at the optimum fitting range. In column 6 are given the optimum fitting range r (in %) and the corresponding value of τ_{end}. Finally, columns 7 and 8 contain the values of the average oscillation frequency $\bar{f}_c = \bar{\omega}_c / 2\pi$ Hz, and the average decay ratio, $\overline{DR}$, with their standard deviations at the optimum fitting range.

The analysis numbers I = 7 and 8 refer to two long records, each containing 54 segments. For a more detailed analysis, the evaluation was at first made at three blocks and then over the whole record length. Block 1 encompasses the segments 1-22 (18 ACFs), block 2 the segments 19-40 (18 ACFs), and block 3 the segments 37-54 (14 ACFs). The signal C2_TEST.L1 shows a transient and the DR is time-dependent. A plot of the values of the oscillation frequency and the DR obtained from the individual ACFs in the GLSA is given in Fig.7, at the optimum fitting range for the whole record length. The indicated scanning time starts with zero at the begin of the record. The signal C2_TEST.L2 is practically stationary.

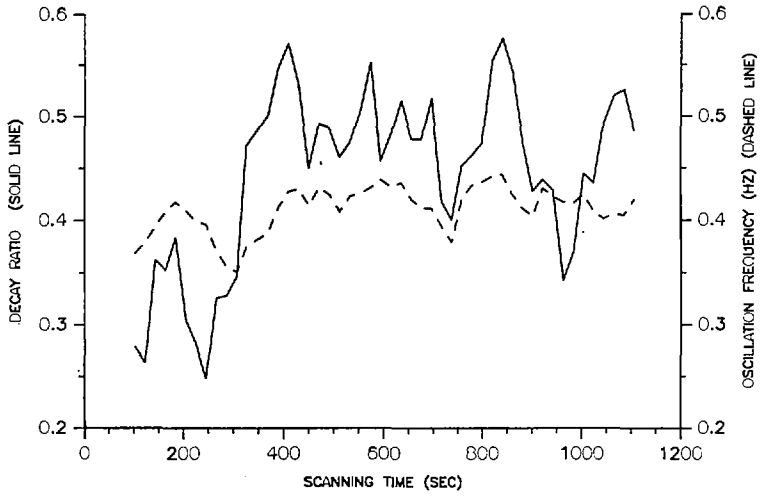

Fig. 7: Decay Ratio (solid line) and Oscillation Frequency (dashed line) in the GLSA of the Benchmark Record C2_TEST.L1 at the Optimum Fitting Range as Functions of the Scanning Time.

5.3 Comparison with Results from Other Methods

For comparison, we summarise in Table 5 the results from 15 other methods. The first line of each analysis case refers to the values of the oscillation frequency, and the second line contains the values of the DR. The data were taken from the benchmark proceedings (Conde et al., 1999), which unfortunately contained no reference to data uncertainties.

Table 5: Benchmark Results

First line: Oscillation Frequency (Hz)
Second line: Decay Ratio

I	Record	M1	M2	M3	M4	M5	M6	M7	M8	M9	M10	M11	M12	M13	M14	M15
1	C1_APRM.1	0.483	0.452	0.487	0.467	0.45	0.350	0.450	0.460	0.460	0.464	0.459	0.459	0.448	0.47	0.458
		0.460	0.423	0.576	0.640	0.42	0.580	0.330	0.500	0.420	0.422	0.460	0.420	0.512	0.57	0.566
2	C1_APRM.3	0.483	0.482	0.481	0.480	0.46	0.270	0.450	0.480	0.490	0.497	0.483	0.483	0.482	0.51	0.476
		0.576	0.582	0.558	0.735	0.30	0.250	0.300	0.500	0.630	0.511	0.537	0.520	0.499	0.60	0.516
3	C1_APRM.4	0.489	0.490	0.487	0.481	0.48	0.280	0.470	0.490	0.460	0.480	0.490	0.490	0.518	0.51	0.490
		0.515	0.514	0.525	0.634	0.39	0.260	0.230	0.530	0.420	0.549	0.528	0.510	0.558	0.78	0.516
4	C1_APRM.12	0.466	0.466	0.467	0.400	0.45	0.300	0.450	0.460	0.460	0.467	0.465	0.465	0.459	0.47	0.452
		0.812	0.809	0.828	0.751	0.68	0.430	0.560	0.780	0.780	0.757	0.792	0.780	0.740	0.66	0.559
5	C2_TEST.S11	0.442	0.440	0.435	0.471	0.410		0.490	0.440	0.420	0.361	0.424	0.424	0.478	0.45	0.444
		0.287	0.268	0.312	0.355	0.360		0.100	0.200	0.200	0.113	0.168	0.150	0.416	0.34	0.580
6	C2_TEST.S31	0.443	0.440	0.437	0.427	0.430		0.410	0.460	0.480	0.482	0.453	0.453	0.478	0.45	0.441
		0.338	0.384	0.475	0.646	0.360		0.190	0.400	0.470	0.323	0.359	0.270	0.416	0.27	0.243
7	C2_TEST.L1	0.454	0.453	0.453	0.472	0.440		0.430	0.450	0.460	0.457	0.444	0.444	0.441	0.45	0.442
		0.395	0.394	0.469	0.432	0.350		0.160	0.350	0.550	0.339	0.360	0.270	0.386	0.23	0.393
8	C2_TEST.L2	0.533	0.533	0.519	0.534	0.500		0.520	0.530	0.510	0.537	0.516	0.516	0.516	0.54	0.516
		0.640	0.640	0.634	0.620	0.570		0.340	0.630	0.600	0.622	0.576	0.570	0.576	0.54	0.534
9	C4_LPRM.8	0.509	0.510	0.507	0.478	0.508	0.400	0.495	0.500	0.510	0.504	0.507	0.507	0.507		0.514
		0.703	0.705	0.694	0.733	0.688	0.740	0.620	0.760	0.710	0.729	0.760	0.700	0.733		0.403
10	C4_LPRM.22	0.530	0.531	0.530	0.557	0.540	0.450	0.495	0.530	0.550	0.512	0.526	0.526	0.523		0.548
		0.583	0.569	0.569	0.702	0.360	0.860	0.380	0.390	0.360	0.422	0.517	0.490	0.447		0.582
11	C6_LPRM.111	0.505	0.506	0.506	0.457	0.463	0.280	0.510	0.53		0.558	0.504	0.504	0.529		0.529
		0.392	0.391	0.382	0.461	0.105	0.280	0.110	0.23		0.277	0.361	0.400	0.344		0.907
12	C6_LPRM.112	0.541	0.542	0.545	0.492		0.250	0.520	0.53		0.520	0.535	0.535	0.517		0.488
		0.413	0.413	0.439	0.362		0.150	0.230	0.20		0.545	0.333	0.320	0.292		0.071
13	C6_LPRM.22	0.519	0.520	0.504	0.528	0.513	0.390	0.510	0.510	0.530	0.471	0.517	0.517	0.513		0.519
		0.384	0.390	0.397	0.589	0.233	0.710	0.200	0.250	0.250	0.332	0.293	0.400	0.357		0.391

14	C6_LPRM.210	0.511	0.512	0.513	0.506	0.496	0.380	0.500	0.500	0.510	0.516	0.501	0.501	0.485	0.494
		0.593	0.594	0.601	0.672	0.302	0.680	0.320	0.510	0.570	0.709	0.513	0.160	0.535	0.473
15	C6_LPRM.211	0.521	0.521	0.521	0.518	0.525	0.310	0.510	0.520	0.520	0.523	0.521	0.521	0.519	0.535
		0.889	0.889	0.890	0.870	0.611	0.450	0.500	0.980	0.950	0.966	0.858	0.950	0.768	0.456
16	C6_LPRM.213	0.521	0.522	0.522	0.519	0.525	0.420	0.510	0.520	0.520	0.524	0.521	0.521	0.520	0.530
		0.897	0.898	0.906	0.876	0.720	0.760	0.530	0.950	0.940	0.935	0.878	0.950	0.836	0.501
17	C6_LPRM.214	0.522	0.522	0.521	0.522	0.511	0.480	0.510	0.520	0.520	0.523	0.521	0.521	0.521	0.523
		0.894	0.896	0.895	0.919	0.766	0.870	0.680	0.820	0.930	0.965	0.877	0.950	0.832	0.425
18	C6_LPRM.215	0.521	0.521	0.522	0.520	0.521	0.480	0.510	0.520		0.524	0.521	0.521	0.521	0.525
		0.963	0.973	0.964	0.966	0.877	0.870	0.780	0.950		0.988	0.954	0.990	0.922	0.495
19	C6_LPRM.218	0.513	0.514	0.514	0.511	0.510	0.250	0.500	0.510		0.498	0.507	0.507	0.454	0.504
		0.547	0.549	0.550	0.700	0.330	0.190	0.420	0.510		0.507	0.503	0.470	0.518	0.590

M1: UPV Standard AR
M2: UPV Full SVD AR
M3: UPV Truncated SVD
M4: UPV Dynamics Reconstruction
M5: Pennsylvania State University
M6: Pennsylvania State University : LAPUR Code
M7: University of Tsukuba
M8: PSI : ARMA Model (Plateau Method)
M9: PSI : AR-AIC
M10: JAERI
M11: SIEMENS AR
M12: SIEMENS RAC
M13: TOSHIBA
M14: TU Delft
M15: CSNNS Mexico

As expected from the fitting sensitivity studies, the fitting procedure with the option IBGR=0 gives primarily a significant underestimation of the DR, combined with a down-shift of the estimated oscillation frequency. This behaviour demonstrates the importance of taking the PSD background term into account. The fitting procedure with the option IBGR=2 shows, in most analysed cases, results which range well within the data obtained by the other methods. However, for high DR cases, one can observe the tendency of a DR overestimation. If one extends the given upper limit of the fitting range up to r = 70 %, then slightly reduced DR values, which are in better agreement, are obtained in most cases.

6. Concluding Remarks

Our method of determining the oscillation frequency and the decay ratio in BWR stability analysis is based on a transparent physical procedure with a simple phenomenological model. The oscillator model B is to be preferred, and has been found to be superior to the oscillator model A. Our procedure is an off-line method. We are still far away from an on-line application.

Our investigations will be a contribution to a problem. The benchmark results reveal that, at present in the field of signal analysis, many different methodologies are used and the uncertainties of the various approaches can differ greatly. In our opinion, the trivial question of which is the best and most reliable method for determining the decay ratio, was not answered by the benchmark project.

The criterion used for determining the optimum fitting range is empirical and may exhibit only one possibility. Further investigations and ideas are desirable.

The space-dependence of the decay ratio is until now not completely understood.

The most important FORTRAN codes mentioned in this paper have now been brought as a package into the MATLAB environment (UNIX operating system), and are there available. Requests for copies should be directed by e-mail to DIETER.HENNIG@PSI.CH.

Acknowledgements

The first author would like to thank Dr. A. Pritzker (PSI) for permission to use the PSI DEC computer system. Both authors are indebted to Dr. T. Dury (PSI) for proof-reading the English text. We also thank Mr. B. Askari (summer student at PSI) for transferring the FORTRAN codes into the MATLAB environment.

References

Askari B., Behringer K. and Hennig D. (2001). Conference paper of M&C 2001, Salt Lake City, Utah, USA, September 2001, CD-ROM.

Behringer K. (1970), Programmbeschreibung der Subroutine MARFIT für einen eindimensionalen Least-Squares Fit von Messdaten mit einer beliebigen Funktion von Unabhängigen Parametern, Internal EIR Report TM-PH-373 (*).

Behringer K. (1988). The Code ACCF1 for Bivariate Correlation Analysis in the Time Domain, Internal PSI Report TM-41-88-06 (*).

Behringer K. (1998), Ann. Nucl. Energy, **25**, 889.

Behringer K. (2001) PSI Report 01-07.

Behringer K., Hennig D. (2002), Annals of Nuclear Energy, 29, 202, 1483-1504

Bendat J. S. and Piersol A.G. (1971), Random Data: Analysis and Measurement Procedures, Wiley-Interscience, New York.

Chen Wai-Kai (1995), The Circuits and Filters Handbook, CRC Press, Boca Raton, Florida.

Conde J.M., Recio M., Verdue G., Ginestar D., Munoz-Cobo J.L., Navarro J., Palomo M.J., Sartori E., Lansaker P. (2001). Forsmark 1 & 2 BWR Stability Benchmark. Time Series Analysis for Oscillation during BWR Stability Operation, Final Report, NEA/NCS/Doc (2001)2.

Guggenheimer J.and Holmes P. (1984), Nonlinear Oscillation, Dynamic Systems and Bifurcations in Vector Fields, Applied Mathematical Sciences, **42**, Springer Verlag.

Hennig D. (1999), Nucl. Technology, **26**, 10.

Kosaly G. (1980), Progr. Nucl. Energy, **5**, 145.

Marquardt D.W. (1963), J. Soc. Indust. Appl. Math., **11**, No. 2, 431.

MATLAB (1992). High-Performance Numeric Computation and Visualization Software, The Math-Works Inc., Natick, Massachusetts.

Moschytz G.S. and Horn P. (1983), Handbuch zum Entwurf aktiver Filter, Oldenbourg.

Thie J.A. (1981), Power Reactor Noise, American Nuclear Society, La Grange Park, Illinois.

Welch P.D. (1967),. IEEE Trans. Audio Electroacoustics, **15**, 20.

(*) Copies of internal EIR or PSI reports are normally available on request from the PSI library.

PAUL SCHERRER INSTITUT

Paul Scherrer Institut, CH-5232 Villigen PSI
Tel. 056 310 21 11, Fax 056 310 21 99
Internet: www.psi.ch